Polymer Flood Management of El Corcobo Norte Using Streamlines

Perea Garcia, M.C.[1], Manfre Jaimes, D.[2], Batycky, R.P.[2], Thiele, M.R.[2]
[1]Pluspetrol, [2]Streamsim Technologies, Inc.

Abstract

Streamline simulation (SLS) offers a powerful method for modeling and evaluating a polymer flood at the field and per-pattern levels. In this paper, we review and discuss the advantages of SLS for polymer flooding as applied to the El Corcobo Norte (Corcobo) oil field in Argentina.

First, we show how to build an ensemble of simulation models that differ in water initialization, oil/water relative permeabilities, and polymer properties to quantify the response uncertainty compared to the historical water and polymer injection responses of the flood. We then use differential evolution (DE) to history match the historical response of wells in the area of interest (AOI) and extract a subset of 40 models to forecast multiple injection and production scenarios to assess the uncertainty in the forecasted response.

Properly designing and managing a polymer flood for an entire field relies heavily on the ability to quantify field-wide remaining oil in place and correctly capture injector-centered patterns due to the high cost associated with injecting polymer. In this paper, we show how forecasted oil response from a streamline-based flow simulation containing +200 injectors and +300 producers, along with an ensemble of history matched models, can be used to calculate pattern incremental polymer injection efficiencies (IPE) and utilization factors (UFs) to determine which areas provide the best economic incremental oil recovery due to polymer injection. We also show how to use the ensemble of models to quantify the impact of lower or higher polymer injection concentrations as another way to optimize polymer injection.

Introduction

Improving oil recovery by adding a polymer to injected water has been discussed extensively in the literature. For a recent discussion on chemical EOR see Delamaide (2020) and references therein. The main physics of polymer flooding centers on increasing the injected water viscosity by adding polymer thereby reducing the mobility ratio and improving the local sweep efficiency. However, ensuring a positive return on investment (ROI) requires tuning a number of design parameters through a combination of laboratory experiments and numerical modeling. In this paper we describe the reservoir flow simulation part of such a design applied to the Corcobo oil field located in the Neuquén Basin, Argentina. In 2018, Hyrc et al. presented an analysis of the same field forecasting a 7% increase in oil recovery compared to pure waterflooding by injecting polymer at 500 ppm for a total rate of 7000 m3/d into 78 injectors affecting 126 producers. The economics were considered attractive and with limited risk.

This work picks up the work of Hyrc et al. (2018) five years later using SLS combined with an ensemble-based workflow (EVOLVE) proposed by Thiele and Batycky (2016).

Corcobo Field

The area is operated by Pluspetrol, including the Jaguel Casa de Piedra and CNQ7 fields (in Mendoza Province, Argentina) and CNQ7A and GAIII fields (in La Pampa Province, Argentina). The productive formations are the Centenario Upper Member (Jagüel Casa de Piedra and Cerro Huanul Sur fields) and Centenario Lower Member (El Corcobo Norte, El Renegado, and Puesto Pinto fields). Both members have similar petrophysical properties. The reservoir is a non-consolidated sandstone with a maximum thickness of 17 m and 600 m depth. It is divided into layers that are either amalgamated or have 2 to 3 m of separation. The permeability varies between 0.5 and 4 Darcies and the porosity between 27 to 33%. The oil is 18° API and has a viscosity in-situ of 160 to 270 cp.

The field development started in 2005. Most of the field has been developed on an inverted seven-spot

pattern with 280-m spacing. Because of the high wettability and the under-hydrostatic pressure (30 kg/cm2 initial), an excellent response to water injection has been experienced. A final recovery factor of 26 to 30% has been estimated. Recovery by primary production has been estimated to be 8 to 10%.

The production mechanism used cold heavy oil production with sand (CHOPS) and the production wells are completed without any restriction for sand production.

Polymers have been injected in a pilot area since 2012, consisting of 6 injectors and their associated producers, at a concentration of 500 ppm. By the end of 2020, polymer injection was expanded to 4 more areas, adding 50 additional polymer injectors.

Modeling Objectives

The objectives of this work were to reassess the incremental recovery potential associated with extending the polymer flood to all wells in AOI—a total of 331—shown in Figure 1.

Figure 1: Location of AOI wells (331) shown in orange in relation to all wells (1527) in the Corcobo field as of 2022. Triangles indicate injectors and dots indicate producers.

Additionally, an important requirement as part of the reassessment was to associate an estimate of the uncertainty associated with every forecast to help quantify the economic risk with an expansion of the polymer flood to all AOI wells.

Streamline-Based Simulation

Streamline simulation as applied specifically to polymer flooding was presented by Thiele et al. (2010) and subsequently applied by AlSofi and Blunt (2010), Clemens at al. (2011), and Choudhuri et al. (2015) among others. A useful collection of papers summarizing the details and application of SLS can be found in SPE's Getting Up to Speed series on Streamline Simulation (2011).

A powerful feature of SLS is the ability to capture injector/producer pairs and their dynamic behavior through time resulting from changes in operating conditions such as well rates and polymer injection concentrations. The benefit of SLS to capture flood metrics has been extensively discussed in the literature and will not be repeated here. The interested reader is referred to references cited in this paper for details and discussions.

One specific metric worth discussing, however, is the utility factor (UF) that is easily extractable on a per-pattern basis when using SLS. The UF is an efficiency metric expressed as the ratio of mass of polymer injected to the oil recovery due to polymer injection incremental to water flooding (Clemens et al. 2011, Zhang et al. 2019):

$$\mathrm{UF} = \frac{\text{mass of polymer injected}}{\text{incremental oil recovery due to polymer}}$$

A reasonable design criterion may be to keep the UF under 3.0kg/STB (19kg/sm3), although there is

no universal consensus on a good threshold. The UF can be translated into an economic efficiency metric but that is dependent on local CAPEX and OPEX costs as well as taxation in order to get a reliable estimate of the net price per bbl of oil produced. In this paper, we prefer to use the incremental polymer efficiency (IPE), which is simply the inverse of the UF: IPE=1/UF. Higher incremental efficiencies imply better use of the polymer which is a more intuitive interpretation of efficiency.

Estimating the incremental oil recovery using traditional modeling approaches can be computed at the field level by doing two forecasts (one with and one without polymer) and then subtracting the two. Estimating the IPE for each pattern, requires as many finite-difference simulations as there are patterns by considering each pattern one-at-the-time. Instead, SLS can efficiently model the entire field and capture the offset oil production associated with each injector by construction and the IPE of all patterns can be calculated with only two forecast simulations—the pure water base case and the polymer injection scenario. The UF can then be used as a screening and optimization metric as it becomes easy to identify inefficient patterns (high UFs, low IPEs) vs efficient ones (low UFs, high IPEs) compared to a desired threshold.

Ensemble Modeling

Using an ensemble of models to forecast allows engineers to generate a probability distribution associated with the forecast predictions, which in turn can help operators manage the risk profile of their portfolios. In this work, we use an ensemble-based modeling approach (Evolve) presented by Thiele and Batycky in 2016.

The Evolve workflow is a linear workflow composed of 4 steps: (1) screening and selection of geological models; (2) calibration of models using field data; (3) calibration of models using individual well data; and (4) economic forecasting. Each step starts with an initial ensemble of models that is reduced to a representative subset of models to use in the next step. For details of the methodology see Thiele and Batycky (2016). Not all 4 steps need to be taken and it is also possible to skip a step. For example, if there is only one geological model available, the initial screening and selection of geological models is not applicable and is skipped. In the specific case of Corcobo, the ensemble of models was built as part of the field-level calibration step of the historical waterflood and polymer flood periods only.

The Corcobo Model

The full-field Corcobo model includes 1078 producers and 449 injectors using a grid of size 253x1171x9 =2,666,367 total cells of which 986,928 are active. Aerially DX=DY=30m while vertically DZ changed to follow the top and bottom of each of the 9 layers as shown in Figure 2. The AOI is outlined in black.

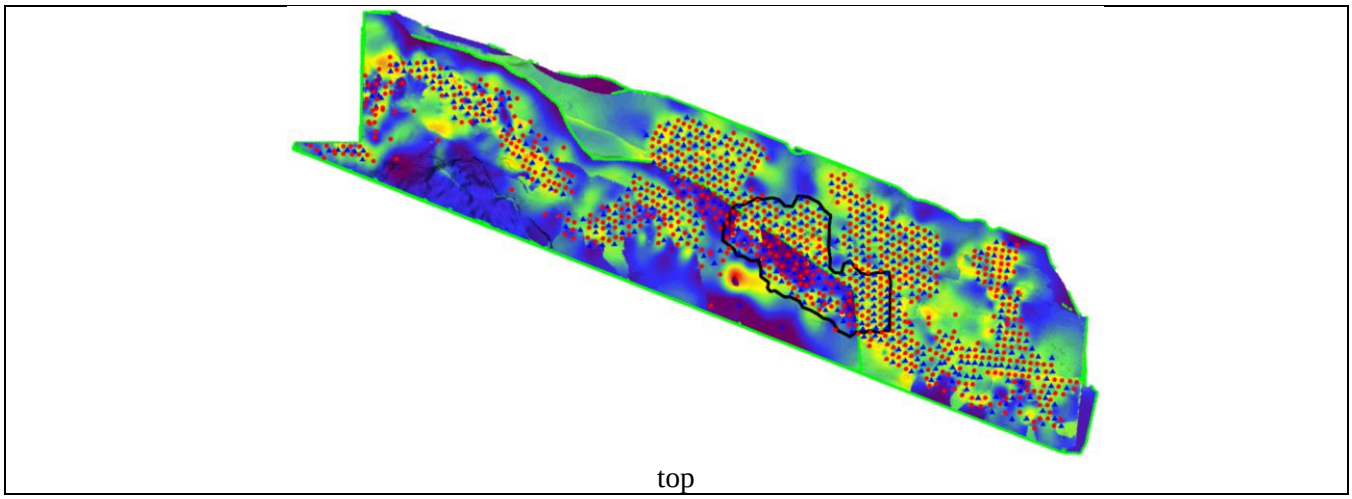

top

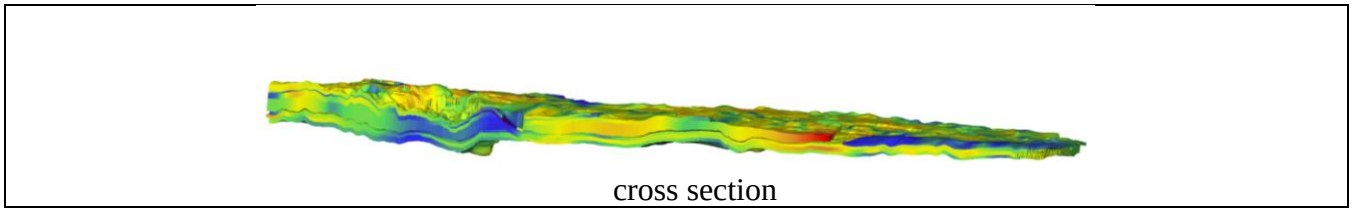

Figure 2: Full Field Corcobo model with 253x1171x9=2,666,367 total cells (986,928 active) including 1078 producers and 449 injectors. Red dots are producers, blue triangles are injectors, and green dots represent open boundaries (not shown in the cross section). The AOI is outlined in black. Color represents initial oil saturation for one realization with red associated with areas of high oil saturation and blue associated with areas of low oil saturation.

To reduce the numerical cost of the study, the full-field model was trimmed to focus on the polymer pilot and areas surrounding the pilot by making regions outside of the AOI inactive as shown in Figure 3. By doing so, the number of active cells in the AOI model is reduced to 277,733. Note that the green dots indicate that the AOI model is open to flow on all four sides. The difference in run times using 4 cores on a 11th Gen Intel Core i9-11950H chip set was 12min for the full field model vs. 3min for the AOI model, a 4x speed-up.

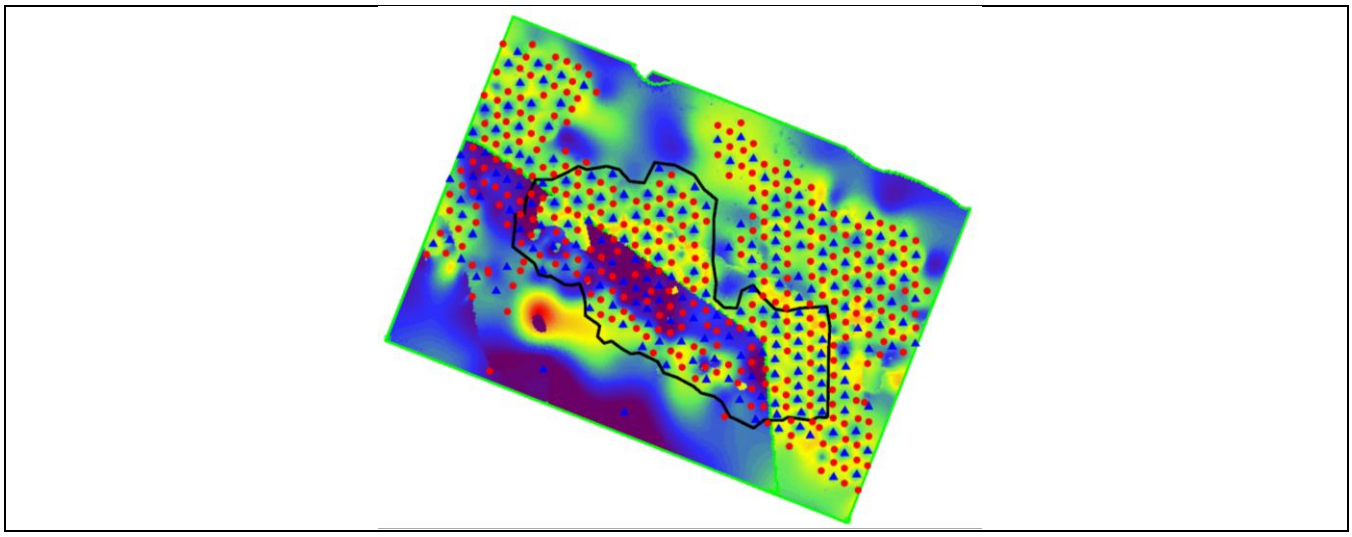

Figure 3: AOI model with the number of active cells reduced to 277,733 from 986,928 leading to a computational speed-up of 4.3 compared to the full field model. Color represents initial oil saturation for one realization.

Creating an Ensemble of Models for the AOI

To create an initial ensemble of 40 models, input from five parameter distributions were sampled using a Latin Hypercube sampler:

Initial oil/water saturation. **The Corcobo AOI model was initialized with saturations maps for each of the 9 layers existing on 2005.10.01. Additionally, layers 7-9 (the prominent layers in the AOI) were modified by introducing eight maximum water saturation upper limits: Swmax=0.15, 0.20, 0.25, 0.30, 0.35, 0.40, 0.45, and 0.50 resulting in a total of 8 possible initial water saturation maps. Oil saturation is then simply $S_o = 1 - S_w$. The variation of water saturation for layers 7-9 is shown on**

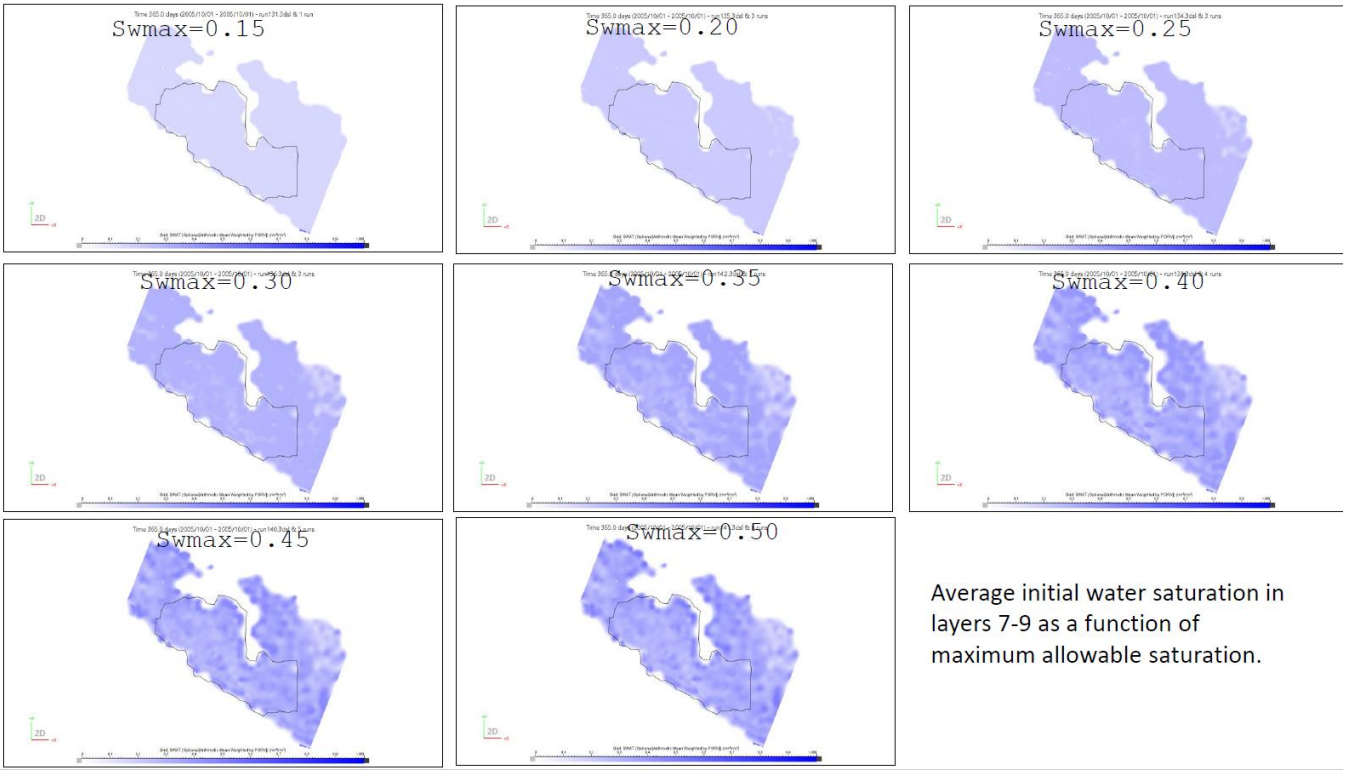

1. Figure 4.

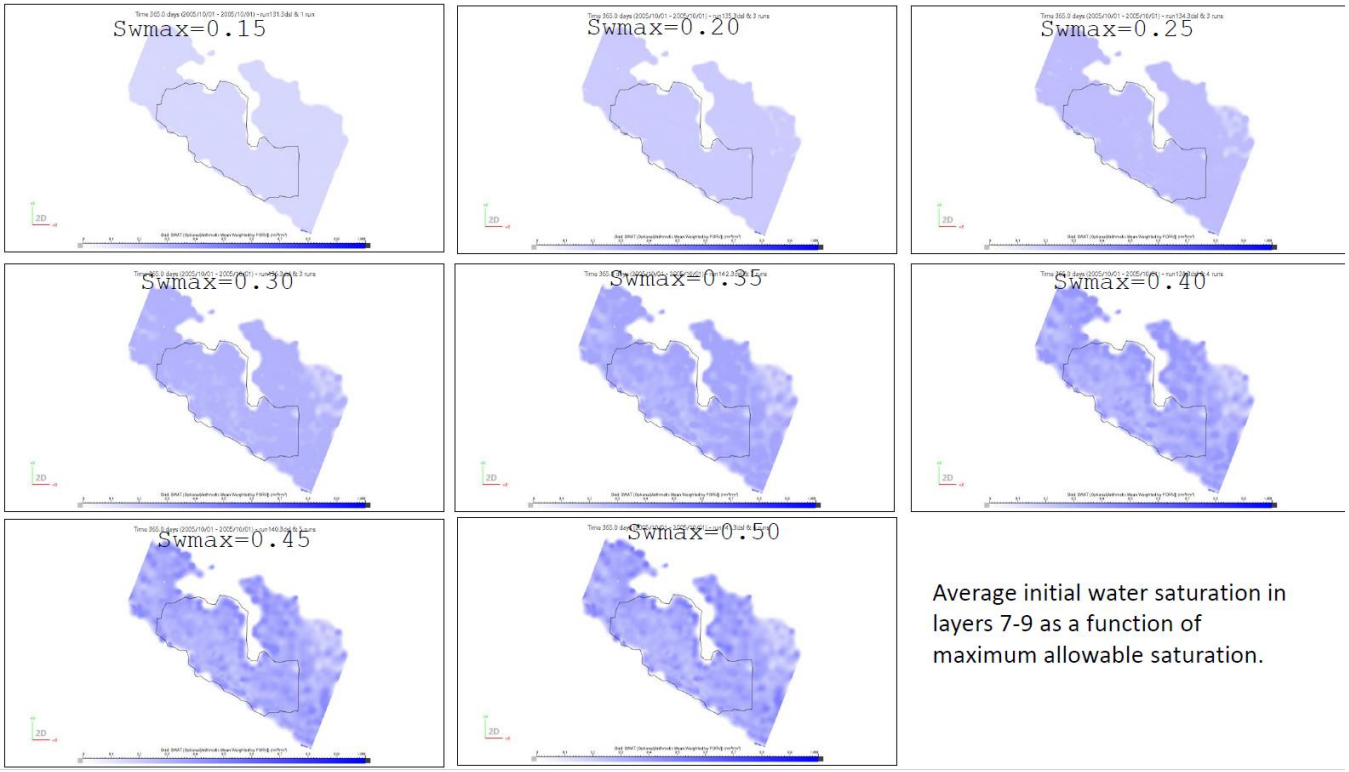

Figure 4: Initial average water saturation distribution in layers 7-9 as a function of maximum allowable water saturation (same color scale [0,1] used for all cases).

2. ***Water connate saturation (SWCO)***. Uniform distribution (0.15 to 0.40)
3. ***Corey oil exponent (oilExp)***. Uniform distribution (0.5 to5)
4. ***Corey water exponent (watExp)***. Uniform distribution (0.5to 5)

5. ***Residual oil saturation to water (SORW)***. Uniform distribution (0.1 to 4)
6. ***Maximum water relative permeability (krwmax)***. Uniform distribution (0.1 to 0.4).

The above six parameter distributions were sampled using Latin Hypercube sampling to create 40 discrete parameter combinations and hence 40 (initial) simulation models. Figure 5 shows the values of the parameters for 10 of the 40 simulation models. For example, the first model (run131) is using the initial water saturation map that has a saturation maximum of 15%, krwmax=0.3176, Corey Oil Exponent=1.405, residual oil saturation is 0.3417, connate water saturation is 0.2281, and a Corey Water Exponent=3.080.

All 40 models were then simulated through the end of history (2022.05.01) to quantify the distribution of oil response in the AOI (Figure 5). For this initial sampling, peak oil rate ranged from almost 5000 m3/day to 500 m3/d. Historical oil production is shown by the green bullets. Given an initial set of 40-parameter combinations, the next step is to use the historical data to reduce the range of the uncertainty in the oil response by updating the values of the parameters. This calibration (history matching) step is done using a global optimization approach called differential evolution (DE).

Differential Evolution

DE is an optimization algorithm (Price et al. 2005) that mimics the process of natural selection and evolution to find the optimal solution using a population of candidate solutions and iteratively improves the solutions over multiple generations. The key steps of DE are (1) initialization, (2) mutation, (3) crossover, and (4) selection of parameter values.

In the initialization step, a starting generation is generated by a random selection from the distributions of each parameter. An important assumption is that parameters are assumed to be independent of each other. The mutation and crossover steps allow to generate new members as well as combine (cross) parameter values of existing members in a generation. Finally, the selection step creates a new generation driven by the objective function.

Runs	krwmax	oilExp	sinit_cuttoff	sorw	swco	watExp
Latin Hypercube 1						
run131	0.3176	1.405	15	0.3417	0.2281	3.080
run132	0.3545	3.006	15	0.2371	0.1843	3.395
run133	0.1484	4.053	30	0.2437	0.2436	2.023
run134	0.1760	1.813	25	0.2046	0.2070	3.264
run135	0.1967	1.953	20	0.2494	0.2485	2.116
run136	0.2106	1.335	30	0.3733	0.3379	0.6521
run137	0.3057	4.626	20	0.3620	0.2976	3.597
run138	0.2694	4.464	40	0.3274	0.2621	4.892
run139	0.1864	2.799	40	0.2129	0.3101	4.370
run140	0.2210	0.6542	45	0.3510	0.2132	3.947

Figure 5: Values of the six sampled parameters for 10 of the 40 initial simulation models.

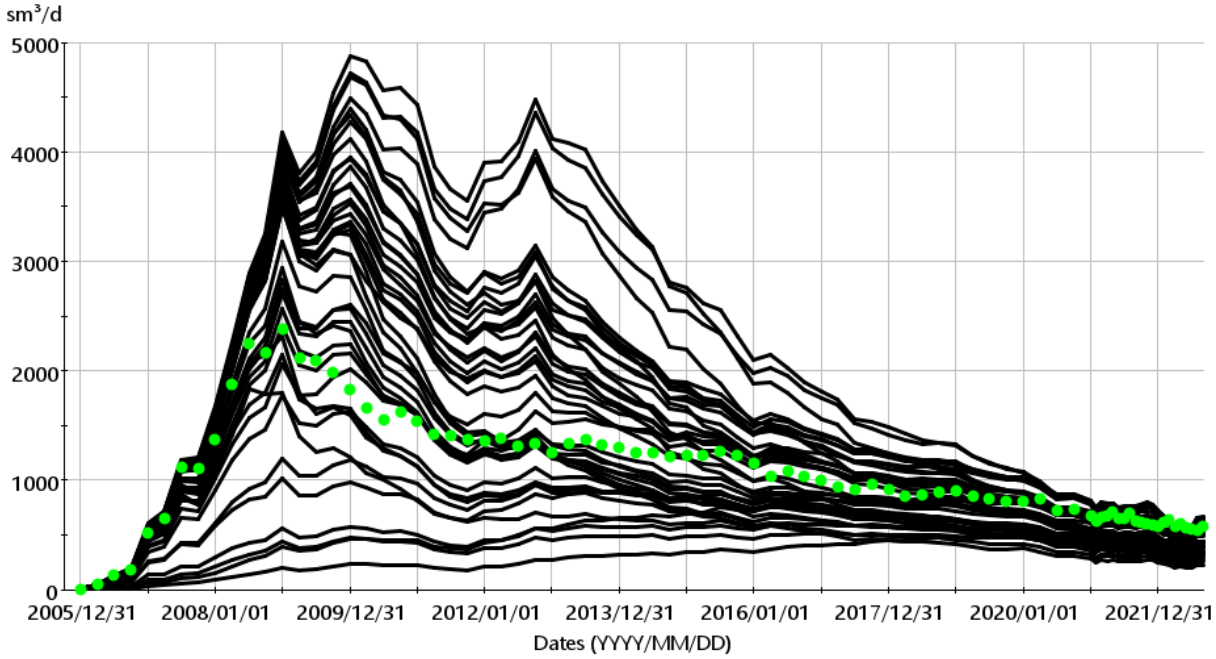

Figure 6: Area of interest wells oil response for the initial 40 simulation models as compared to the historical oil rate (green dots).

AOI Level Waterflood History Matching from 2005 to 2012

The first step in the calibration of the AOI is to focus on the waterflood period (2005-2012) prior to polymer injection. The global objective function used as part of DE is the sum of mismatches in each well's oil rate, $Q_{o,w}$ at every timestep i across all 231 producers in the AOI from 2005 to 2012 as shown in Eq 1.

$$OF = \sum_{w}^{231} \sum_{i}^{nt} \Delta t_{i,w} \times \left| Q_{o,w,i}^{sim} - Q_{o,w,i}^{hist} \right|$$

Next, we applied DE over 7 generations to update each of the six parameters and improve the waterflood history match of the 40-model ensemble. Figure 7 shows the AOI daily oil rate response for the 40 models at the end generation 7. Notice how the spread in oil rate has been reduced compared to Figure 6 for the history matching period and beyond the history matching period, although this late period was not explicitly used in the calibration step. This is expected since most of the AOI wells remained on waterflood from 2012 to present.

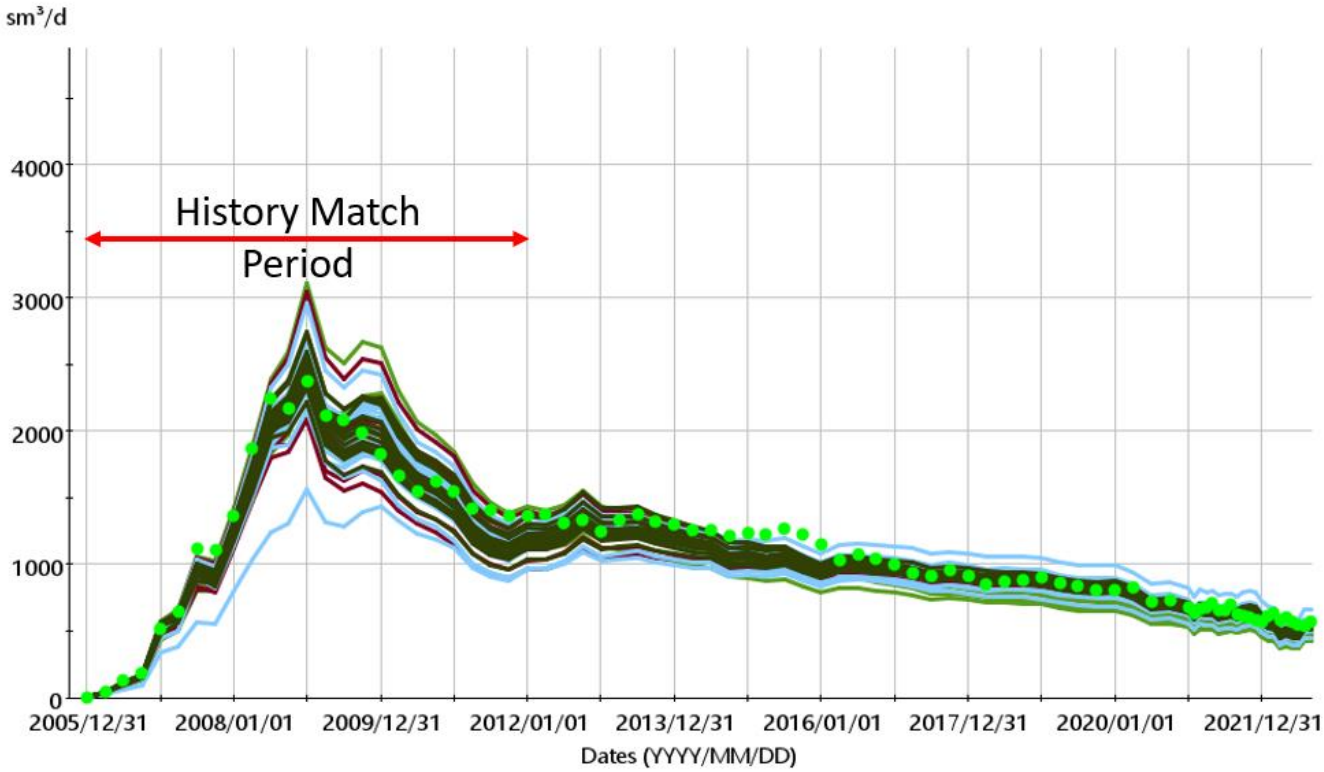

Figure 7: Daily oil rate for the AOI wells for generation 7 (40 models) after applying differential evolution to improve the waterflood only history match.

During each generation, it is possible to display how the distribution of each of the six parameters changes as part of the global optimization steps (generations). For example, there were 8 equally probable initial water distributions with the maximum saturation cutoff ranging from 15% to 50% (vertical axis of Figure 8) but by generation 7 two models had a cutoff of 20%, six models had a cutoff of 30%, and one model each for a cutoff of 45% and 50%. The distribution of the points in generation 7 shows that the cutoff of 25% has the highest posterior probability, meaning the it is the most likely value given the historical data and the parameter distributions associated with the relative permeability curves for oil and water. A summary of the remaining parameters for generation 7 is shown in Figure 9. For example, while the initial distribution of residual oil saturation (Sorw) in column one of Figure 7 ranged from 0.2 to 0.4, the final generation range was reduced to 0.2 to 0.26.

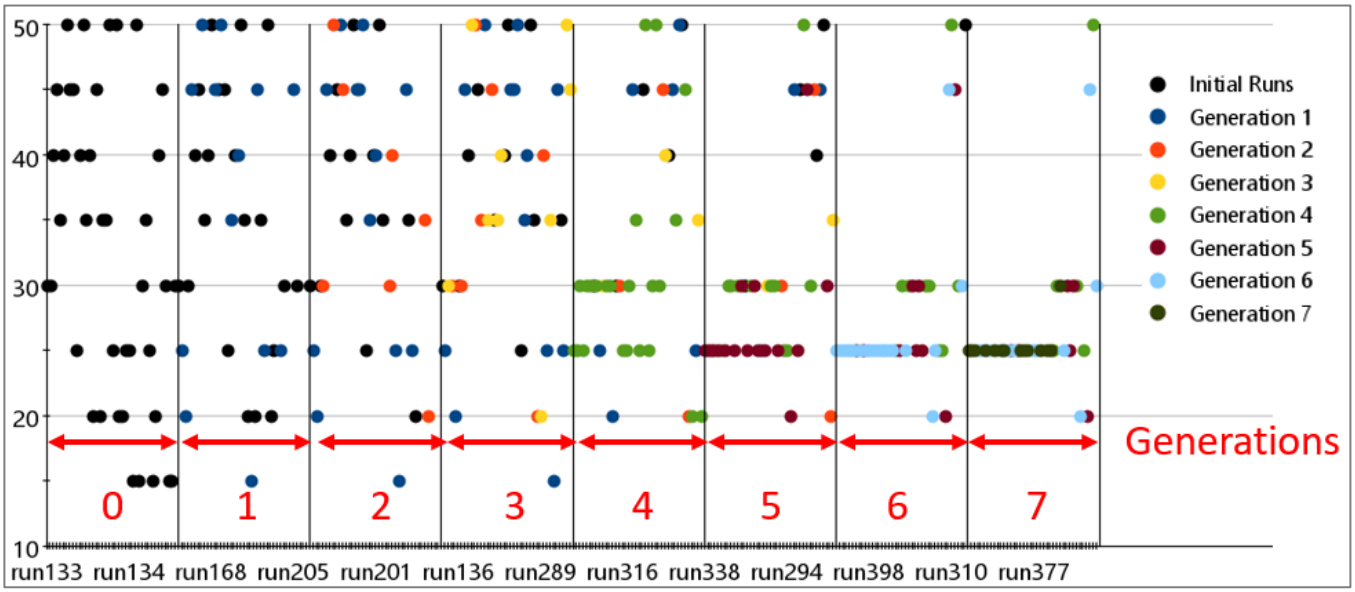

Figure 8: Distribution of the models by their water saturation cutoff within each generation. By generation 7, the 25% cutoff model is the most probable, while models with cutoffs of 15%, 35%, and 40% did not survive. Colors represent the generation in which a model was introduced.

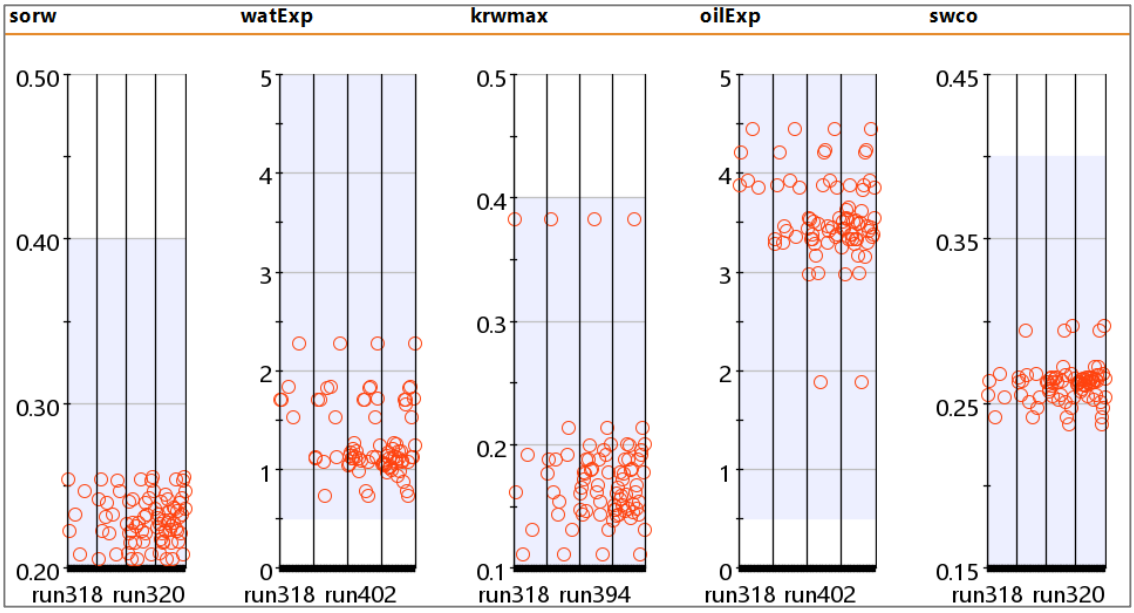

Figure 9: Combinations of the other five parameters values at the end of generation 7 resulting in the ensemble of models for the AOI and associated oil rate match for the waterflood period shown in Figure 7.

Polymer Injection Pilot History Matching from 2012 to present

Polymer injection started in 2012 in 6 injectors in a pilot area in the center of the AOI using an injection concentration of 500ppm in each injector. To model the polymer displacement physics, the reservoir simulator input parameters include (1) the water viscosity multiplier as a function of polymer concentration; (2) inaccessible pore volume (IPV); (3) maximum polymer adsorption; (4) water relative permeability reduction factor (RRF); and (4) polymer shear thinning. For the purpose of calibrating the

oil rate polymer response, only the first 3 parameters (viscosity multiplier, IPV, and maximum adsorption) were assumed to have a substantial impact on the oil rate. The ranges used for the polymer parameters were chosen as follows.

1. A table of effective water viscosity vs polymer concentration was defined for a range of concentrations from 0 to 1400ppm. Next five different multipliers to the effective water viscosities in the table were defined as 0.2x, 0.5x, 1x, 2x, and 5x. This input was in the form of 5 tables of effective water viscosities vs polymer concentrations.
2. The IPV ranged from 0 to 0.3 with a uniform distribution.
3. The maximum adsorption ranged from 1E-9 kg.ply/kg.rock to 1E-2 kg.ply/kg.rock in powers of 10 (8 values).

These three new parameters were sampled along with the 10 parameter combinations resulting in the lowest objective function for the water flood period (10 best runs from generation 7 above). As in the previous case, we again extract 40 new parameter combinations across the four new parameters (three polymer parameters plus one parameter representing the combinations of the 10 best runs from the waterflood period) to use in DE and calibrate against the polymer flood period.

We define an objective function similar to Eq 1 although the well list now only includes 33 producers within the pilot area that are offset to the six polymer injectors. The time frame is from 2012 to present. Figure 10 shows the oil response for the pilot area across 40 new models representing the initial generation in DE. For these models, polymer response begins about 1 year after polymer injection with some models showing overly optimistic response compared to history while other models show minimal response to polymer injection.

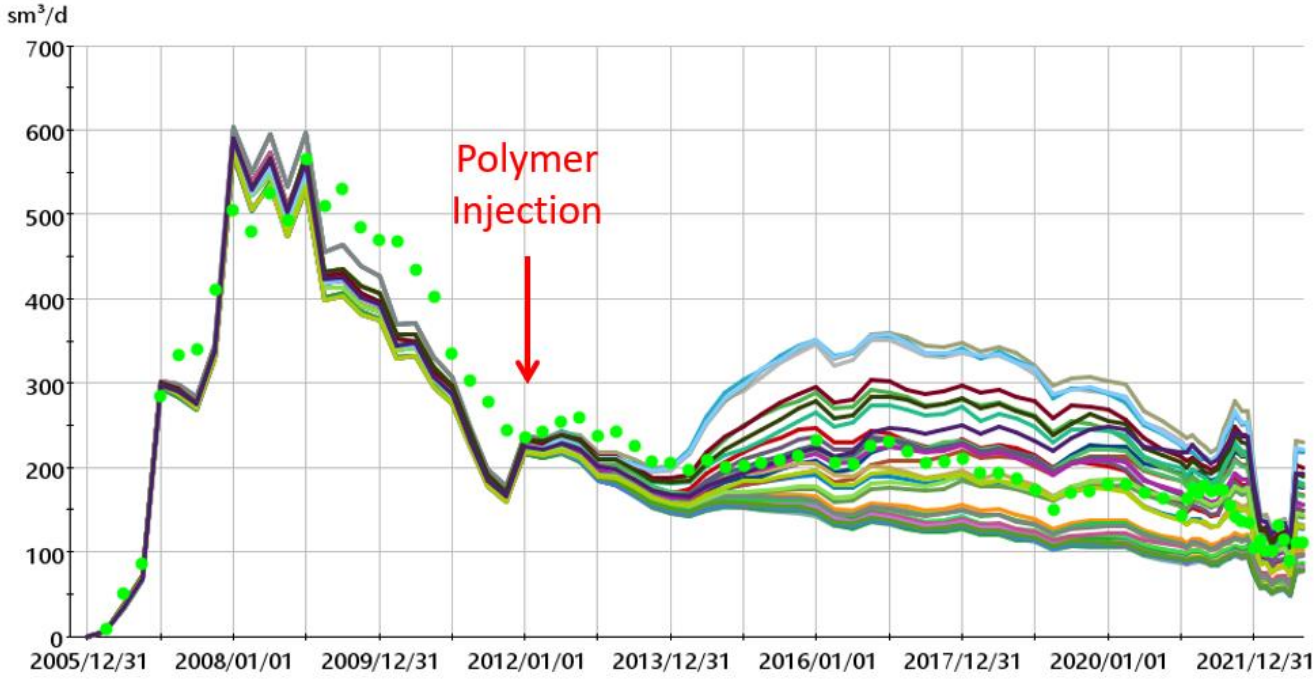

Figure 10: Oil rate for polymer pilot area producers for 40 new models that have variability in both waterflooding and polymer flood simulation parameters. Polymer injection was started in 2012 to present.

To calibrate the polymer flood response against the historical data, five generations of DE were used. Figure 11 shows the parameter evolution across the 5 generations. For example, the multipliers to the effective viscosity vs. polymer concentration of 0.2x and 5x were eliminated by generation 5 (left image), while the range on IPV was only slightly reduced from 0.0-0.3 (in gen0) to 0.0-0.24 (in gen5) while for

the waterflood matched parameter combinations (right most picture), there were 10 combinations for gen0 while only 8 combinations survived by generation 5 with combinations #8 and #9 having the highest probability. Note that only 5 generations were used as reduction in the objective function showed little improvement after generation 4.

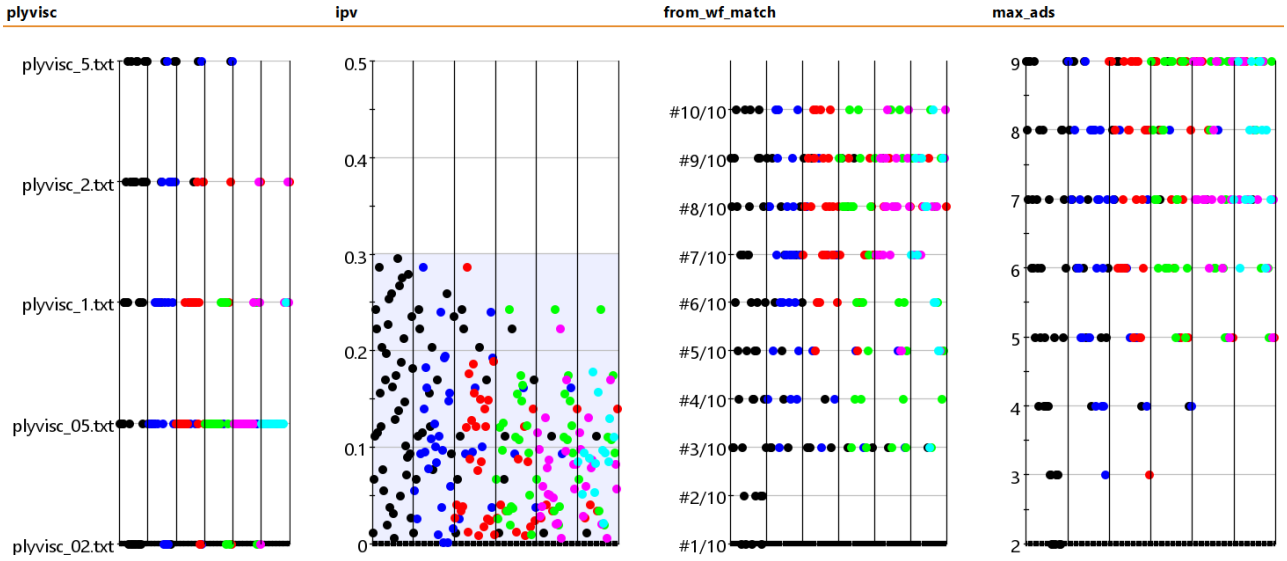

Figure 11: Distribution of the 5 parameters and their values for the initial generation and 5 subsequent generations. Each generation's new and surviving values are represented by a unique color (gen0=black, gen1=blue, gen2=red, gen3=green, gen4=purple, gen5=lightblue)

The final generation ensemble's oil rate response is shown in Figure 12. Note that the initial oil rate (pre polymer injection) is low compared to history. This is because the waterflood history match was performed using an objective function of all wells in the AOI level not just on the subgroup of wells used in Figure 12. Post polymer injection there is clearly an impact of the polymer parameters, as seen by the large range in oil responses. Due to this low initial oil rate in the ensemble, the cumulative oil production of the ensemble (for the pilot area wells) is slightly low compared to the historical cumulative. This also means that the remaining oil in place in the pilot area is somewhat optimistic which may result is overly optimistic forecasts in the next section of the paper.

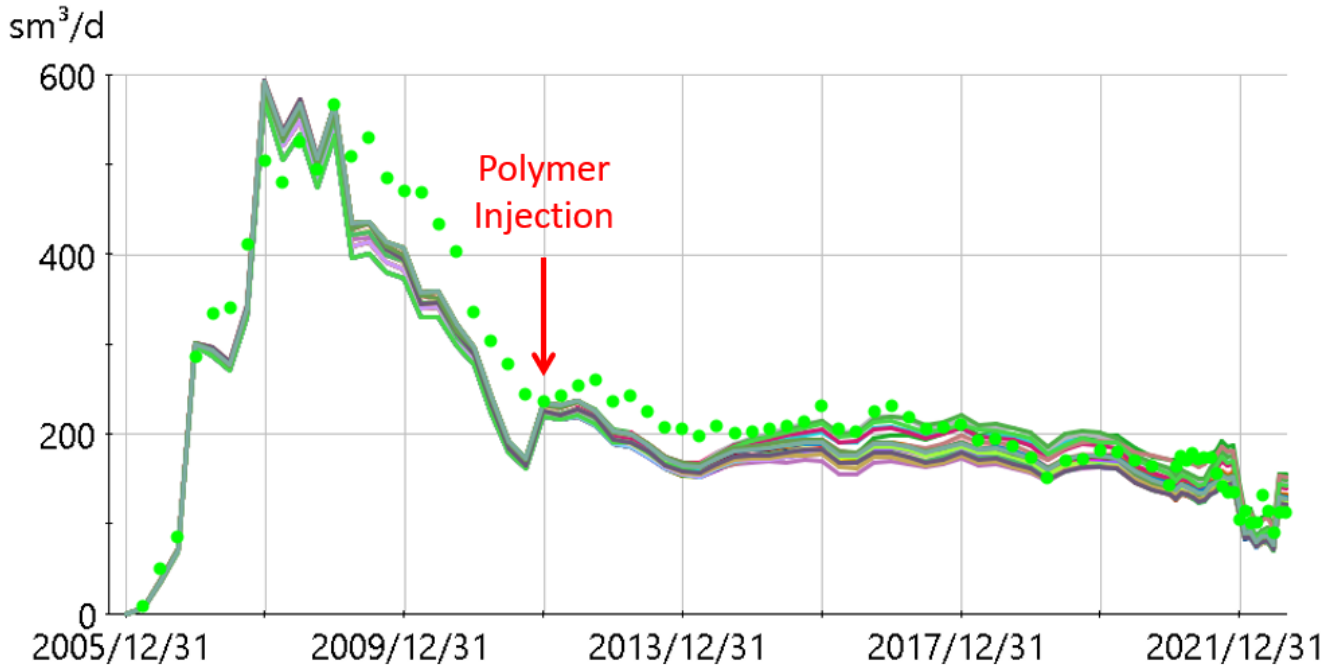

Figure 12: Oil rate for polymer pilot area producers across the 40 model ensemble of generation 5 of differential evolution.

At this point we now have an ensemble of 40 models with 40 unique parameter combinations from both the waterflood match of the AOI wells and the polymer flood match of the pilot wells. Recall that the history matches are at a well group level. Individual wells have not been history matched. One obvious next step would be to history match each of the 40 models at the individual producer level, but this would be done by modifying local geology (porosity and permeability) between well pairs, rather than modifying global parameters. As this remains an expensive and time-consuming task, this step is skipped for now. Skipping the individual well calibration implies that forecasts using the 40 model ensemble may be reliable at the AOI and pilot group level but not necessarily at the per injector pattern or producer level.

Forecasting & Optimization

Forecasting the Polymer Pilot Area

As with all polymer injection schemes, incremental oil response due to polymer injection will decline over time, and a valid question to ask is "When to stop injecting polymer?" Here we answer this question by simulating two forecast scenarios for the final ensemble of 40 models: (1) a base case scenario where polymer injection remains at 500ppm; and (2) a scenario where the polymer injection concentration is set to zero. Injectors are set to their final water injection rate at the end of history, in order to eliminate the decline in injection rates, and hence offset production rates, as total injection mobility decreases with additional polymer injection. Producers are set to their last BHP control at the end of history to allow for minor rate changes to the producers as polymer is flushed out of the reservoir. These two sets of forecasts are shown in Figure 13 for the pilot area producers for a 10 year forecast period. Notice that there is no difference in the two ensemble forecasts initially, which is expected as there is a time lag on polymer injection oil response. However, by Y2024 continued polymer injection is better than reverting to water-only, indicating that oil response is still benefiting from polymer injection. This forecasting process should be repeated ever year to justify ongoing polymer injection versus reverting to water-only injection.

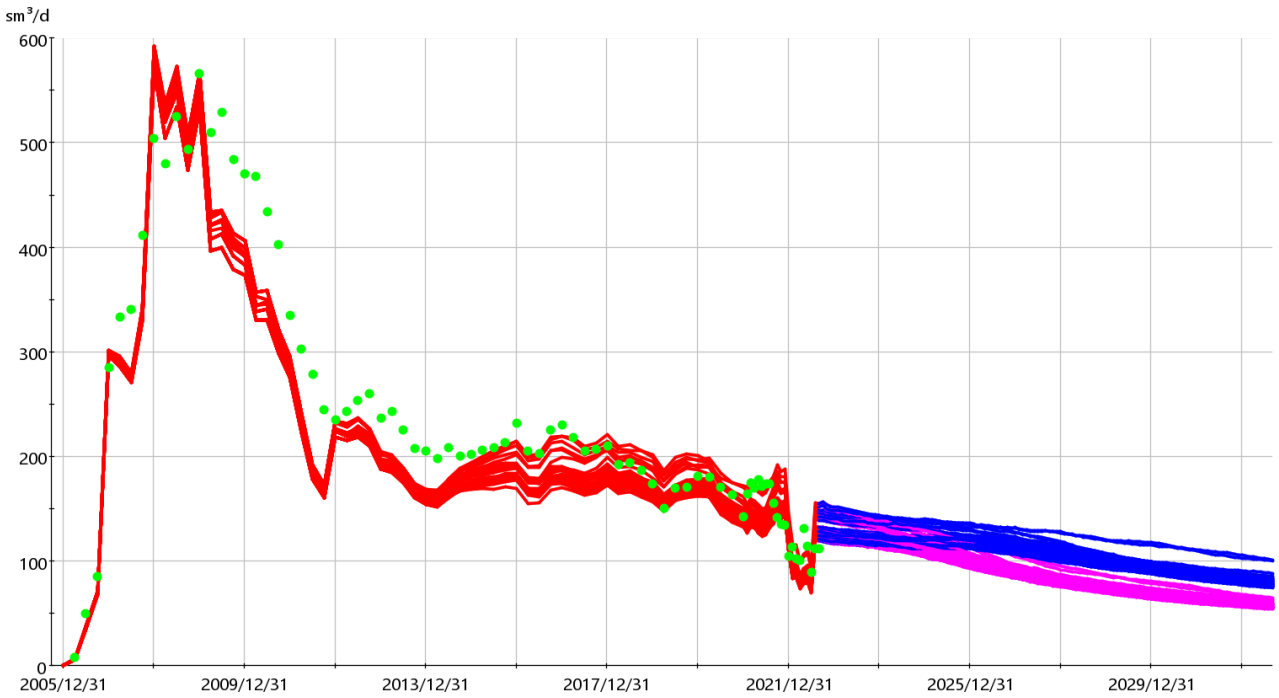

Figure 13: Polymer pilot area 10 year forecast across the 40 model ensemble for continued polymer injection (blue) and reverting to waterflood-only (pink).

For the polymer pilot area we can also quantify the incremental response due to continued polymer injection for this ensemble by first subtracting the polymer forecast scenario response from the water-only response for each forecast scenario pair (a pair has the same simulation input parameters), repeating for all forecast pairs and then displaying as incremental oil response vs time for all runs in the ensemble. Figure 14 shows a probabilistic representation of the oil response of the 40 models, where the incremental cumulative oil response due to continued polymer injection after 10 years ranges from a value of 61100 (P10) to 78220 sm3 (P90) with an expected value of 67400 sm3. Also shown in Figure 14 is a summary of the IPEs for the pilot area across the ensemble at the end of the forecast. Incremental efficiencies range from a low of 0.055sm3/kg (UF=18kg/sm3) to a high of 0.070sm3/kg (UF=14kg/sm3) with an expected value of 0.060sm3/kg (UF=16 kg/sm3). The IPE can be used when comparing new injectors or well groups to roll out polymer to or when comparing which injectors within the current group have incremental efficiencies lower or higher within the pilot group. Recall that due to the slightly optimistic amount of remaining oil in the pilot area, these incremental efficiencies for the ensemble are assumed to be optimistic.

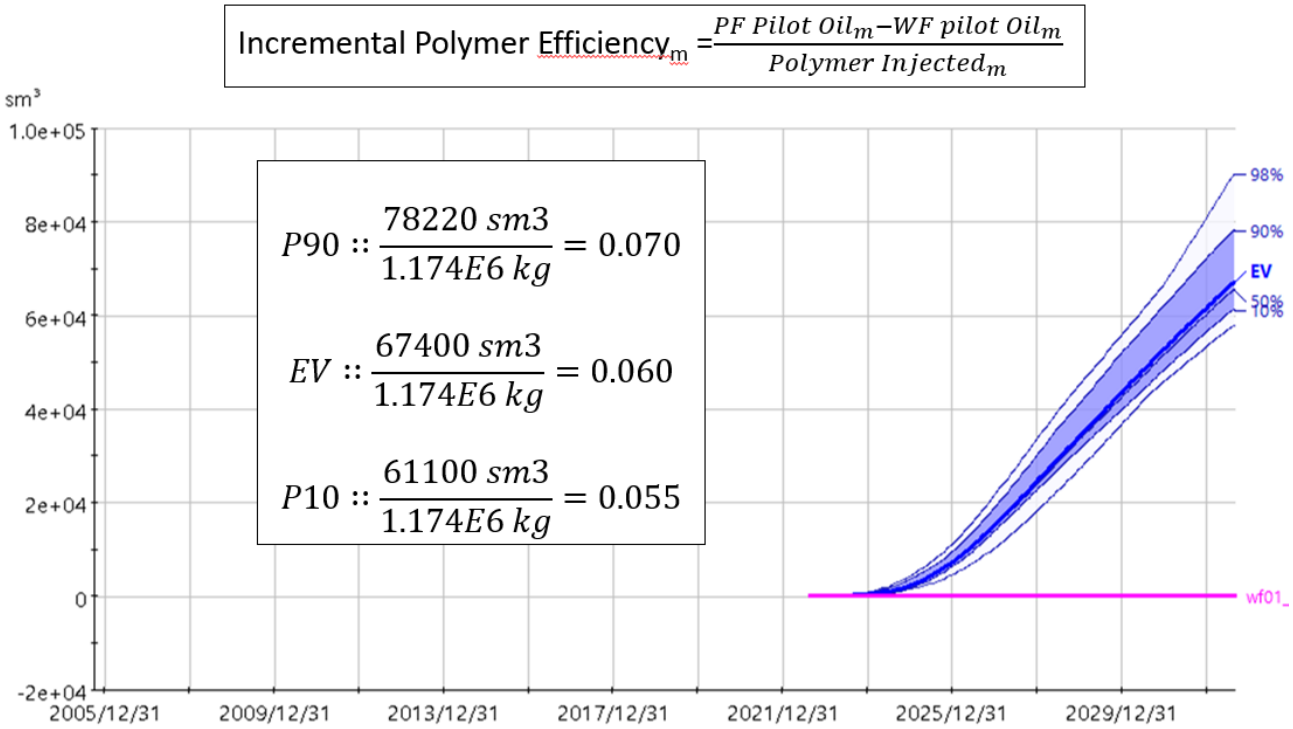

Figure 14: Incremental cumulative oil response for the pilot area for a 10 year forecast for all 40 models. Incremental polymer efficiency is computed for the P10, EV, and P90 responses.

Forecasting the New Polymer Injection Area

Most of this field is not under polymer injection, but the success of the pilot area shows that incremental oil response due to polymer is achievable. Indeed, polymer injection was rolled out to 50 more injectors in late 2020.

Using the approach described in this work, it is possible to rank the response of polymer rollout across the remaining five subgroups in the AOI. Figure 15 shows the 10-year incremental forecast scenario (incremental to reverting back to pure water injection) for a different group of injectors and their offset producers. As with the pilot area, we want to quantify the benefit of polymer injection compared to water-only injection, which can be summarized by computing the IPE. In this case the incremental polymer efficiency ranges from 0.029 (UF=34kg/sm3) to 0.040sm3/kg (UF=25kg/sm3).

It is also worth comparing the performance of the new area to the pilot area performance. Here, incremental efficiency is less than the current pilot area even though the pilot area has had more than 10 years of polymer injection to date. This is expected because the remaining oil in place at the end of the history match for the pilot area—although slightly optimistic due to the less than satisfactory history match in the pilot area—is substantially larger than the remaining oil in place for this new area, even after the polymer injection to date. Given the higher incremental efficiency of the pilot area, the implication is that if an operator only had a finite amount of polymer to inject then the recommendation would have to be to continue polymer injection in the pilot versus rolling out to this new group of injectors.

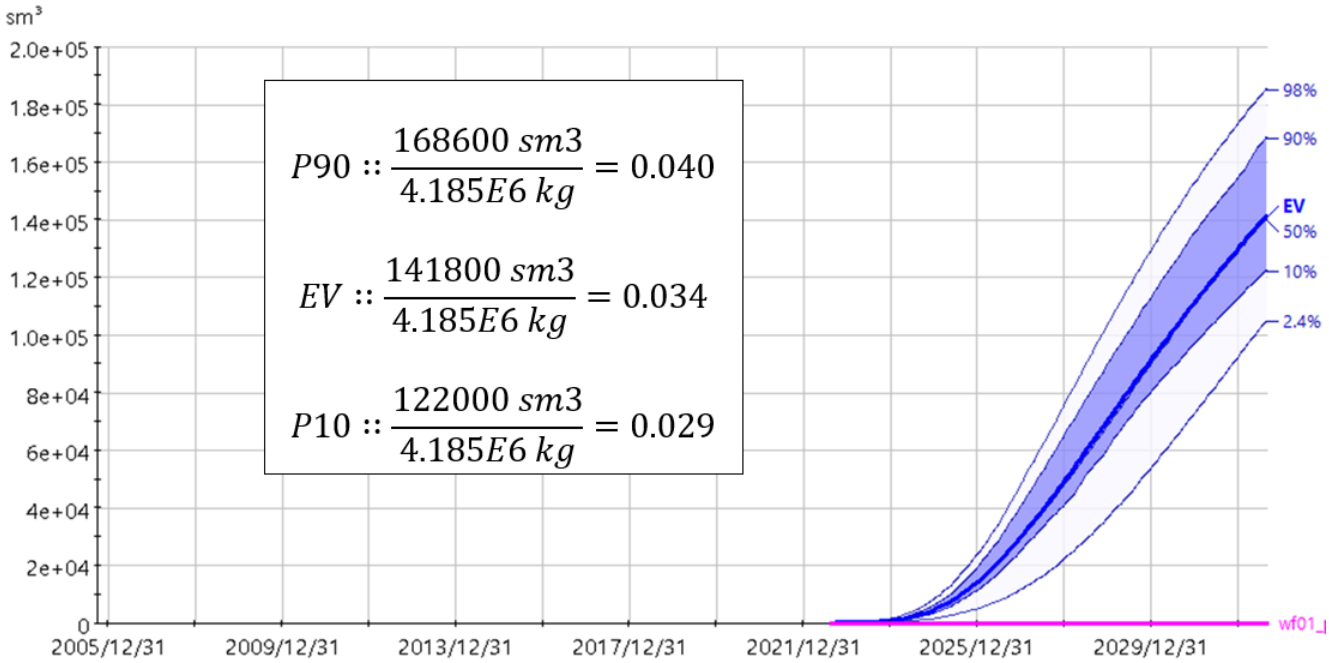

Figure 15: Incremental cumulative oil production of a new polymer injection area for a 10 year forecast for all 40 models. Incremental polymer efficiency is computed for the P10, EV, and P90 responses.

Forecasting Oil Response to Polymer Injection Concentration

In this section we consider the impact of polymer injection concentration on the existing pilot area. Current polymer injection in the pilot area is 500 ppm although surface facilities will allow up to 1500 ppm. We consider 9 injection concentration scenarios ranging from 0 to 1500 ppm for the 6 injectors in the pilot area. All other injectors in the AOI remain on their current injection rates and concentrations (800 ppm), which is the same base case forecast of the previous section. Furthermore, to eliminate the reduction in water injection rates (and production rates) due to injectivity declining with increasing polymer concentration, all injectors for all forecast scenarios were set to maintain their latest injection rates over the 10 year forecast. By keeping injection rates constant any changes in oil production are only due to changes in displacement efficiency of the polymer. We then subtract the cumulative oil production of the zero ppm injection case from each of the other injection concentration forecast scenarios, for each of the 40 models. Figure 16 shows the incremental cumulative oil produced for each of the 40 models for the 800 ppm case relative to the zero ppm case. Notice that the incremental oil production for each model is close to zero for the first two years suggesting that the injected polymer response on oil rate takes about two years. Next, each scenario ensemble is represented as a probabilistic distribution with P10, expected value (EV), and P90 values to calculate the IPE range at 800 ppm. These steps are repeated for each injection concentration scenario and summarized in Figure 17. The expected value of IPE (orange dots) increases slightly as injection concentration increases, meaning that incrementally there is continued benefit to increased concentrations (ignoring injectivity issues) up to the maximum of 1500 ppm. Note too that the range of uncertainty on the IPE decreases as ppm increases which is due to the larger absolute incremental oil recoveries relative to the spread in oil recovery, particularly at very low ppm's.

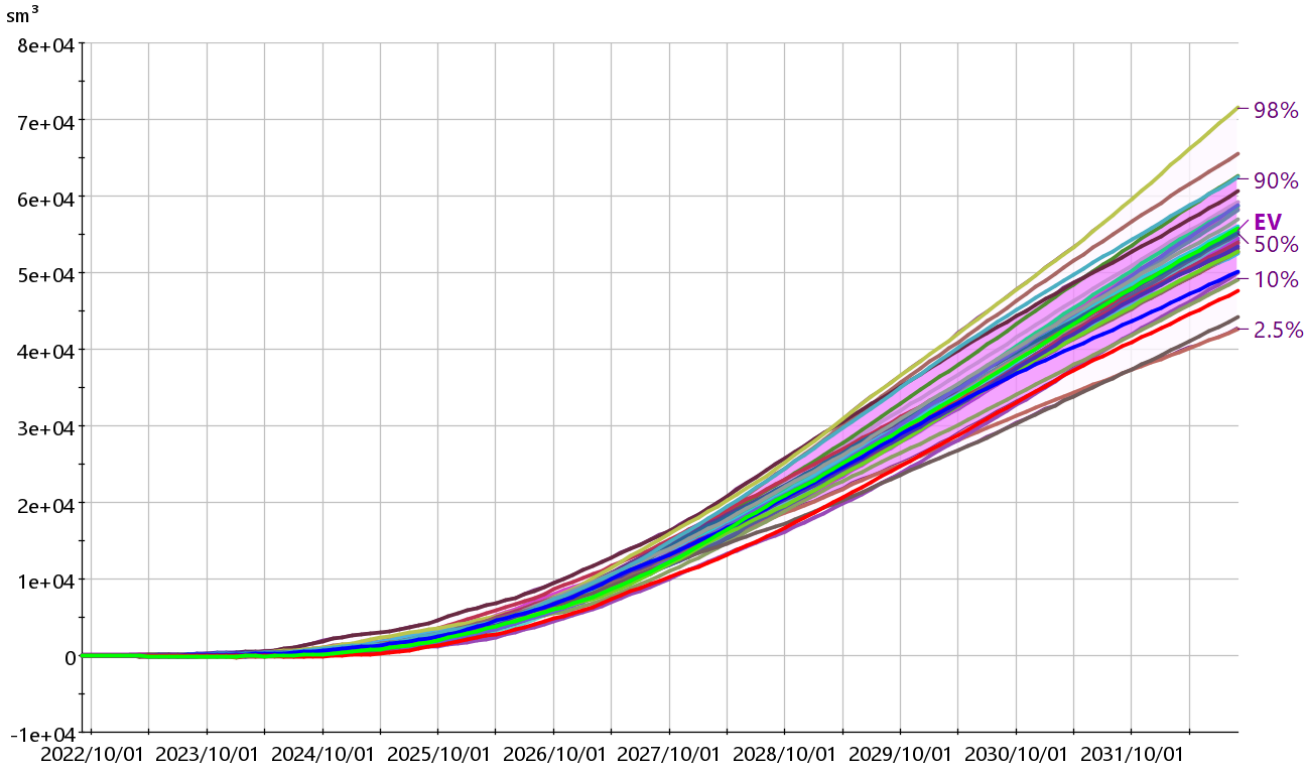

Figure 16: Incremental cumulative oil produced for the 800 ppm scenario relative to the 0 ppm scenario for the pilot area for all 40 models. Labels are for the probabilistic representation of the ensemble.

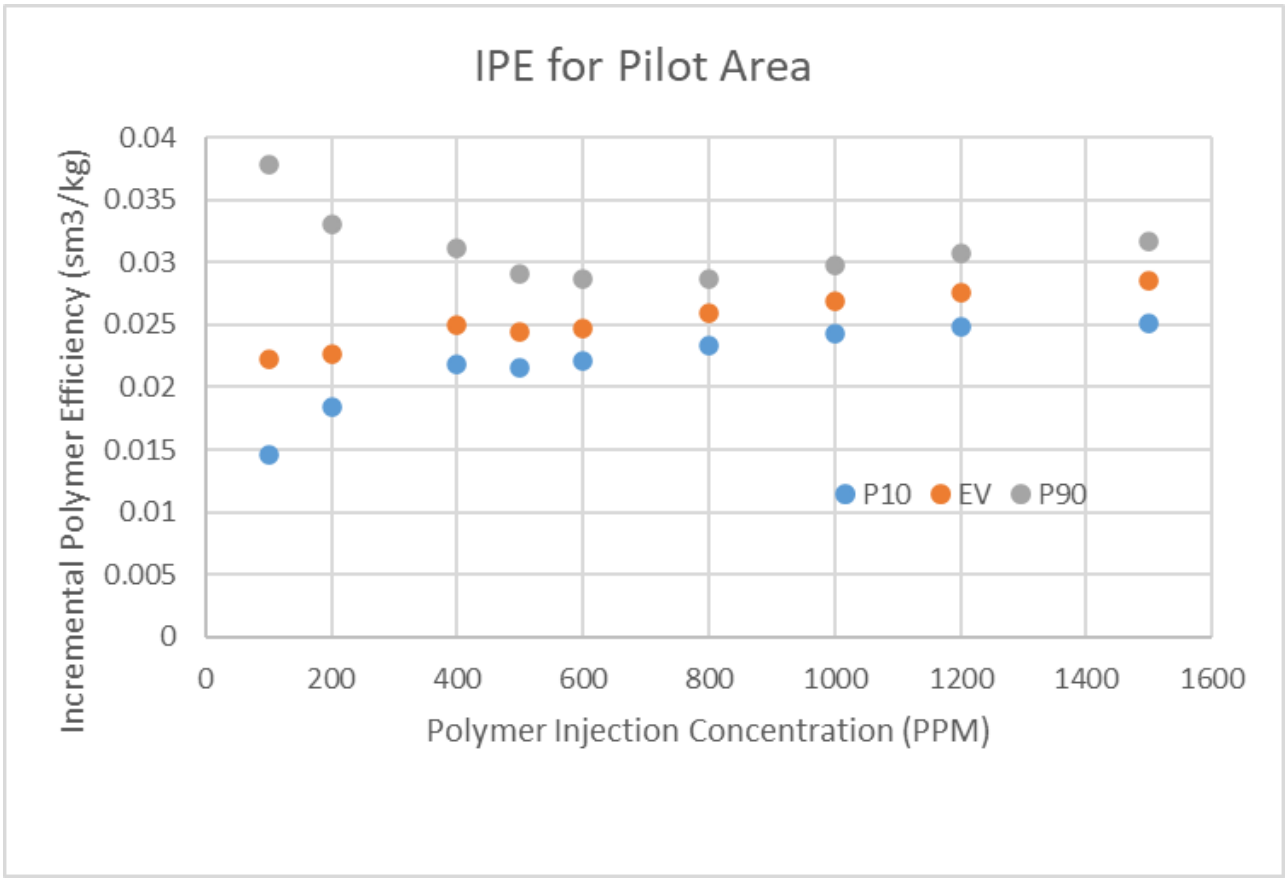

Figure 17: Incremental Polymer Efficiency (IPE) for the pilot area injectors relative to a water only (0 ppm) injection scenario as a function of polymer injection concentration. At each injection

concentration value, 40 models were forecasted, and the P10, expected value, and P90 of the incremental cumulative oil was determined, which then gave the IPE values.

The final step in the forecast analysis is to convert each scenario into economic numbers. Here we calculate incremental net present values (NPV) relative to the pure water (0 ppm) injection case assuming an oil price of US$60/bbl, US$3/kg of polymer, US$1/m3 water processing cost, at an 10% discount rate and 6% inflation rate. We ignore any taxes or royalties. In all scenarios, total water injection rate is the same, and well count is fixed, meaning that we can ignore all other operating costs when computing incremental numbers as these will cancel out. The incremental NPV numbers are shown in Figure 18 and suggest that increasing polymer injection concentration results in an almost linear increase in incremental NPV. The linear increase is expected since the IPE is almost constant for any injection concentration. Recall, however, that changes in injection and production rates with a decreasing injectivity (increasing PPMs) are not accounted for. Decreasing injection and production rates with increasing PPMs would have a significant impact on incremental NPV values.

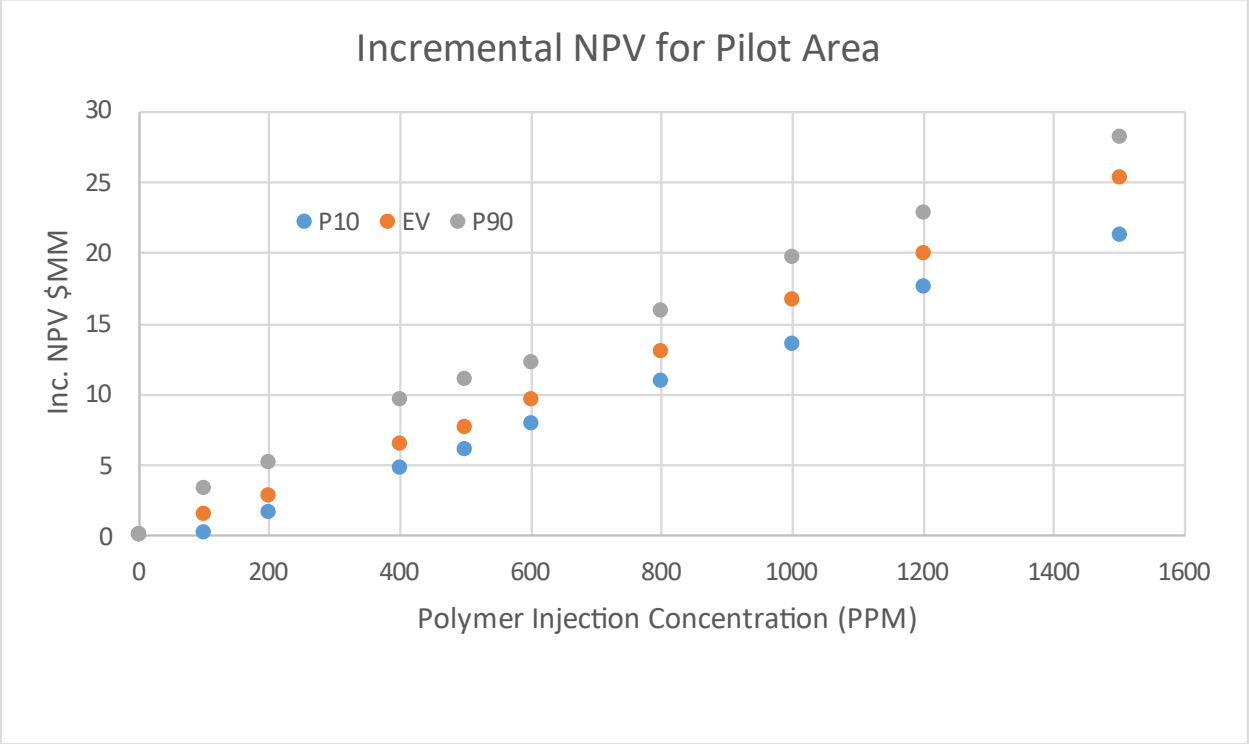

Figure 18: Incremental NPV, relative to the no polymer injection case (0 ppm), for the pilot area for different polymer injection concentrations.

Discussion

There are other forecast scenarios that can be considered with the 40-model ensemble. For example, when increasing the polymer injection concentration in the pilot area, we could have included both reduced injectivity and productivity effects, and then compute new incremental efficiencies and compare those to the current forecasted efficiency in the pilot. Or, similar to the pilot area, we can test optimal polymer injection concentrations in each new area to quantify if incremental efficiencies can be improved compared to the results of Figure 15.

As with different polymer efficiencies between different injector areas (pilot area vs new area), there are different efficiencies even within the pilot area at the per-injector pattern level. Choudhuri et al. 2015

showed such results for a mature polymer flood in Oman, clearly showing that some patterns were no longer responding to continued polymer injection while other patterns were forecasted to continue to have good response. Key to their results, although only based on a single reservoir model, was that their model was history matched at the individual well level. In other words, a next step with this 40-model ensemble will be to quantify the quality of the well-level history match, and then if needed improve the matches via changes at the per-model and per-well level.

Conclusions & Recommendations

Polymer flooding is a viable option for Corcobo with a positive economic return for all areas considered in this study. Using an ensembled based modeling approach, the 10-year economic forecast of the original pilot area remaining at 500ppm polymer injection concentration shows an incremental (compared to reverting back to pure waterflooding) expected NPV of 8 US$MM and associated uncertainty range given by a P10 NPV of 6 US$MM, and a P90 NPV of 11 US$MM.

For all cases considered here, the higher the polymer injection concentration the higher the economic return, suggesting that the single most important constraint to economic return is injectivity of individual wells.

From a modeling perspective, the forecasted economic return is principally a function of the remaining oil in place (ROIP) at the start of forecasting and the injected concentration used to displace the ROIP. For this study, the models were calibrated using the historical response of the well groups associated with various areas, rather than individual wells. A calibration effort using individual well responses would likely yield a more reliable ROIP map and NPV forecast of each model in the ensemble and should be considered in future work.

Another improvement recommended for future work is to include geological variability as an additional parameter when building an ensemble of models. Having more than one geological model would significantly improve the quantification of the uncertainty associated with the expected NPV.

References

AlSofi, A.M. and Blunt, M.J. 2010. Streamline-Based Simulation of Non-Newtonian Polymer Flooding. SPEJ **15** (4): 895-905. SPE-123971-PA. https://doi.org/10.2118/123971-PA.

Chiotoroiu, M., Peisker, J., Clemens, T., and Thiele, M.R. 2017. Forecasting Incremental Oil Production of a Polymer-Pilot Extension in the Matzen Field Including Quantitative Uncertainty Assessment. SPE Res Eval & Eng **20** (4): 894-905. SPE-179546-PA. https://doi.org/10.2118/179546-PA.

Choudhuri, B., Thakuria, C., Belushi, A.A., Nurzaman, Z., Hashmi, K., and Batycky, R.P. 2015. Optimization of a Large Polymer Flood With Full-Field Streamline Simulation. SPE Res Eval & Eng **18** (3): 318-328. SPE-169746-PA. https://doi.org/10.2118/169746-PA.

Clemens, T., Abdev, J., and Thiele, M.R. 2011. Improved Polymer-Flood Management Using Streamlines. SPE Res Eval & Eng **14** (2): 171-181. SPE-132774-PA. https://doi.org/10.2118/132774-PA.

Delamaide, E. "Is Chemical EOR Finally Coming of Age?" Paper presented virtually at the SPE Asia Pacific Oil & Gas Conference and Exhibition originally scheduled to be held in Perth, Australia, 20–22 October 2020. https://doi.org/10.2118/202276-MS.

Hryc, A., Hochenfellner, F., Ortíz Best, R., Maler, S., and Freedman, P. “Development of a Field Scale Polymer Project in Argentina” Paper presented at the SPE Improved Oil Recovery Conference held in Tulsa, Oklahoma, USA, 14-18 April 2018. https://doi.org/10.2118/190326-MS.

Price, K.V. Storn, R.M., and Lampinen. 2005. Differential Evolution: A Practical Approach to Global Optimization (Natural Computing Series). Springer-Verlag, Berlin, Heidelberg.

Thiele, M.R. and Batycky, R.P. "Evolve: A Linear Workflow for Quantifying Reservoir Uncertainty" Paper presented at the SPE Annual Technical Conference and Exhibition held in Dubai, UAE, 26-28 September 2016. https://doi.org/10.2118/181374-MS.

Thiele, M.R., Batycky, R.P. Poellitzer, S., and Clemens, T. 2010. Polymer Flood Modeling Using Streamlines. SPE Res Eval & Eng **12** (2): 313-322. SPE-115545-PA. https://doi.org/10.2118/115545-PA.

Thiele, M.R., Gerritsen, M., and Blunt, M.J. Streamline Simulation. 2011. Getting Up To Speed Series, SPE.

Zhang, Z., Datta-Gupta, A., and Delshad, M. "History Matching and Optimal Design of Chemically Enhanced Oil Recovery Using Multi-Objective Optimization" Paper presented at the SPE Reservoir Simulation Conference held in Galveston, TX, 10-11 April 2019. https://doi.org/10.2118/193860-MS.